

# Development and Validation of Linear Alternator Models for the Advanced Stirling Convertor

Jonathan F. Metscher<sup>1</sup> and Edward J. Lewandowski<sup>2</sup>  
NASA Glenn Research Center, Cleveland, OH 44135

Two models of the linear alternator of the Advanced Stirling Convertor (ASC) have been developed using the Sage 1-D modeling software package. The first model relates the piston motion to electric current by means of a motor constant. The second uses electromagnetic model components to model the magnetic circuit of the alternator. The models are tuned and validated using test data and compared against each other. Results show both models can be tuned to achieve results within 7% of ASC test data under normal operating conditions. Using Sage enables the creation of a complete ASC model to be developed and simulations completed quickly compared to more complex multi-dimensional models. These models allow for better insight into overall Stirling convertor performance, aid with Stirling power system modeling, and in the future support NASA mission planning for Stirling-based power systems.

## Nomenclature

ASC	=	Advanced Stirling Convertor
$B_r$	=	residual magnetic flux density (T)
BOM	=	beginning of mission
$K_i$	=	alternator motor constant (N/A)
EM	=	electromagnetic
EOM	=	end of mission
$F$	=	Force (N)
FringeMult	=	Sage fringe effect multiplier
HR	=	high reject temperature
$I$	=	current (A)
$J_{Sat}$	=	saturation magnetic polarization (T)
$J_{mult}$	=	Sage magnet strength multiplier
$L_{alt}$	=	alternator inductance (H)
LR	=	low reject temperature
$N$	=	number of turns
PM	=	permanent magnet
$Q$	=	net heat input (W)
$R_{alt}$	=	alternator resistance ( $\Omega$ )
$R1, R2$	=	resistances ( $\Omega$ )
$Sage_{Q_{in}}$	=	net heat input as calculated by Sage (W)
$V_{emf}$	=	electromotive force (EMF) voltage (V)
$W_{net}$	=	Power (W)
$x$	=	position (m)
$\mu_r$	=	relative magnetic permeability (N/A <sup>2</sup> )
$\Delta V$	=	voltage (V)
$\Phi$	=	magnetic flux (Wb)

---

<sup>1</sup> Coop Student, Thermal Energy Conversion Branch, 21000 Brookpark Rd.

<sup>2</sup>ASRG Project Lead Engineer, Thermal Energy Conversion Branch, 21000 Brookpark Rd., AIAA Senior Member.

## I. Introduction

STIRLING technology development<sup>1</sup> is continuing at the NASA Glenn Research Center (GRC) as an efficient and reliable power system potentially for NASA's deep space missions. Currently, when radioisotope power is required, NASA deep space missions use radioisotope thermoelectric generators (RTGs), which convert the heat from radioactive decay of Plutonium-238 into electric power, but they have efficiencies of 5 to 7 percent. Stirling engines are a higher-efficiency alternative that could significantly reduce the amount of material used in radioisotope power systems by a factor of 4 or more.<sup>1,2</sup>

The Advanced Stirling Converter<sup>3,4</sup> (ASC), developed by Sunpower, Inc., is a free-piston Stirling engine coupled with a linear alternator. The ASC is currently under extended testing at GRC.<sup>5,6</sup> It is a reciprocating resonant system that consists of a helium filled pressure vessel containing a piston, displacer, and linear alternator. Electrical power is extracted in the linear alternator where the reciprocating piston motion drives magnets through the alternator coil. Figure 1 is a cross section view of a generic free-piston Stirling convertor and defines the main components.

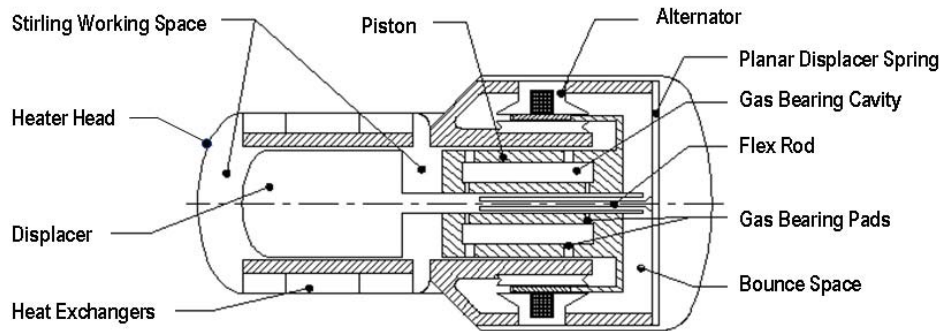


Figure 1 : ASC Cross Section Layout

### A. ASC Modeling

Modeling and simulation is important in the development and testing of Stirling engines as it aids in optimization of design, analysis of system performance, and understanding of physical parameters that are impractical to measure in Stirling devices. There have been both one-dimensional (1-D) and multi-dimensional modeling and simulation efforts focusing on the ASC. One-dimensional models use nodes to directly solve the governing system equations and are advantageous due to their fast computation times and ease of setup.<sup>7</sup> One-dimensional models such as the System Dynamic Model<sup>8</sup> (SDM) enable whole convertor simulation by linking representative elements within the Simplorer™ commercial software package. SDM also has capability of modeling transient startup and non-linear dynamic behavior, although this makes it more computationally intensive. SDM is limited by less sophisticated Stirling cycle thermodynamics and a simplified alternator model. Sage is another 1-D modeling package that is used to model Stirling engines. It is a steady state modeling package that is less computationally intensive and has been continually improved over the years. Its thermodynamic computations have been shown to agree well with 2-D computational fluid dynamic (CFD) models.<sup>9,10</sup> Recent additions to the Sage model library allow for modeling of linear motors and alternators, enabling whole convertor modeling of the ASC. Further detail on Sage and validating its modeling capability is discussed later in this paper.

Multi-dimensional simulations are typically CFD models that focus on specific regions of the Stirling engine such as the regenerator, although there has been some work toward whole engine modeling.<sup>7</sup> Multi-dimensional simulations offer many advantages as outlined by Dyson<sup>11</sup>, such as modeling inherently 3-D phenomena as flow turbulence. Multi-dimensional simulations are computationally expensive and do not typically include linear alternator modeling to give a whole convertor simulation. The ANSYS Maxwell finite element method (FEM) software package allows multi-dimensional modeling of the linear alternator and has been used at GRC to model linear alternator designs from earlier Stirling convertor efforts.<sup>12</sup> Maxwell has the same disadvantage of being computationally expensive and not able to model the whole convertor.

A whole convertor model would be beneficial in analyzing test data as it enables the simulation of parameters that are impractical, if not impossible, to measure and assists in system verification and validation. This paper reviews a whole convertor modeling effort using the Sage software package. As a 1-D model, it will allow for fast

development and simulation times. Simulations are compared to test data to validate the model and determine model limitations.

### B. Sage Overview

Sage<sup>13</sup> is a 1-D Stirling device modeling software package developed by Gedeon Associates. Sage contains a library of generic model components that can be placed and connected in the Sage graphical user interface (GUI). The model components contain the user-defined dimensions and properties and are connected to other model components through various connection interfaces (force, pressure, volume flow, heat flow, etc.). Sage components can be thought of as building blocks that are assembled to form the system of interest.<sup>14</sup> Figure 2 shows an example of Stirling engine components and their interconnections. Components may then have sub-components and their own connections. This modular method facilitates quick model construction as the underlying equations are defined by the components and their interconnections. Sage allows the user to optimize parameters according to defined constraints and optimization objectives. This powerful ability enables design optimization or can assist in tuning model parameters using performance data.

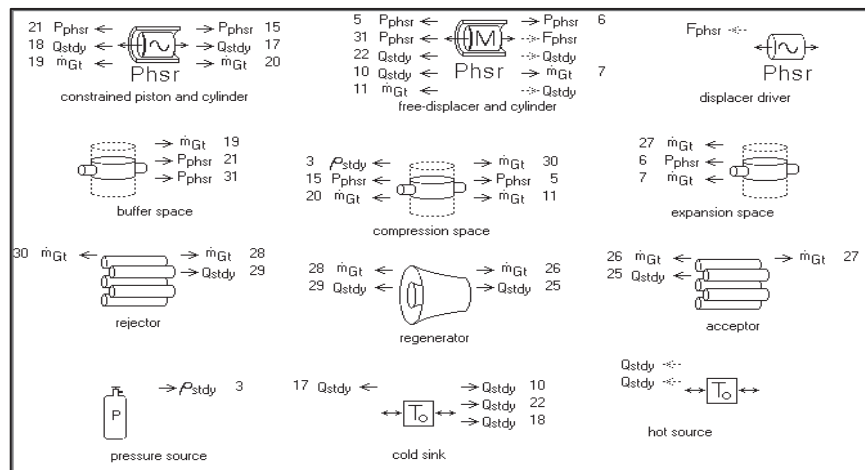
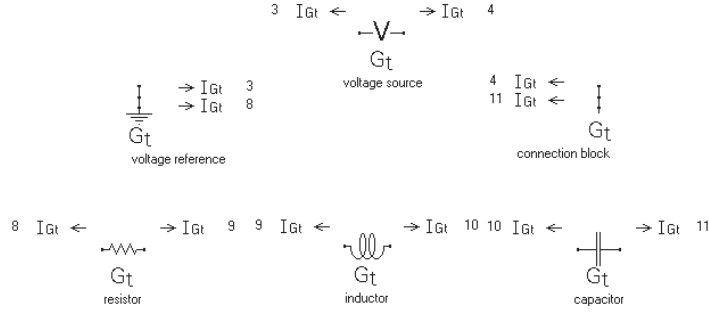


Figure 2: Sage Stirling engine model.

The Sage library is divided into model classes (Stirling, Pulse Tube, and Low-T Cooler). The Stirling model class has been used for modeling ASC engines, but until recently was unable to model the linear alternator. The recent addition of electromagnetic (EM) components to the Sage library allows the modeling of simple circuits and linear motors and alternators, enabling whole convertor modeling of the ASC.

The Sage EM library consists of basic circuit components as well as magnetic components. It includes resistor, capacitor, and inductor model components as well as voltage and current sources. Component properties are user-defined and the components are connected through current interfaces. These components can be used to model simple RLC circuits as shown in Fig. 3, or used as part of more complex EM models and combined with magnetic model components.



**Figure 3: Example RLC circuit model in Sage.**

The library also includes a wire coil that can be used with magnetic model components to develop linear electric actuator and generator models or similar devices such as transformers. The library contains magnetic components such as magnetic field or flux sources, air gaps between magnetic components, permanent magnet (PM) and ferromagnetic materials, and magnetic single- or two-pole components. EM components are connected through magnetic flux ( $\phi$ ) interfaces. Some of these high-level components have built-in sub-components to further define the model structure. The user defines the physical dimensions of the components, however it should be remembered that this is a 1-D model and the geometry is assumed axisymmetric. The solution is also time-periodic and does not model transient behavior, making this unsuitable for certain system simulations or analyses.

### C. Linear Alternator Operation

A linear alternator operates on the principle of Faraday's law in which an electromotive force (emf), or voltage, is induced along the boundary of a surface through which there is changing magnetic flux.<sup>15</sup> In the case of the ASC linear alternator, permanent magnets are attached to the piston which oscillates within the alternator coil. The magnetic field ( $B$ ) from the magnets is directed across the pole gaps and through the inner and outer ferromagnetic cores, following a path of least reluctance ( $\mathfrak{K}$ ) much like current through circuit follows a path of least resistance. As the piston moves through one cycle, the magnetic flux changes as its path changes. The magnetic flux passing through the alternator coil will increase and decrease in an oscillatory manner due to the changing position of the magnets within the stationary ferromagnetic cores, causing the magnetic field to change direction. This changing magnetic field passing through the circular surface enclosed by the alternator coil causes a voltage to be induced ( $V_{emf}$ ). Equation (1) shows Faraday's law in its integral form. Magnetic flux ( $\phi$ ) is the integral of the magnetic field through a surface (Eq. (2)) and the magnetic flux through each "surface" created by the turns ( $N$ ) of the alternator coil are known as flux linkages ( $N\phi$ ).<sup>16</sup>  $V_{emf}$  can be simplified as the time derivative of the flux linkages (Eq. (3)).

$$V_{emf} = -\frac{d}{dt} \int \vec{B} \cdot \hat{n} da \quad (1)$$

$$\phi = \int \vec{B} \cdot \hat{n} da \quad (2)$$

$$V_{emf} = -N \frac{d\phi}{dt} \quad (3)$$

$V_{emf}$  is in phase with piston velocity; however, the voltage at the alternator terminals ( $V_{alt}$ ) is phase shifted due to the inductance of the coil and acts to oppose changes in current. This behavior stems from Lenz's law in which the direction of the induced current in the coil flows as to create a magnetic field opposing the change in magnetic flux through the coil. Inductance ( $L$ ) is defined in Eq. (4)<sup>17</sup>. Sage takes a slightly different approach at calculating

inductance (Eq. (5))<sup>14</sup> but can be shown to be consistent by substituting the relationship between voltage and inductance shown in Eq. (4).

$$L = \frac{d\phi}{dI} = -\frac{V_{emf}}{\frac{dI}{dt}} \quad (4)$$

$$L = -\frac{\phi \Delta V * \dot{I}}{\phi \dot{I}^2} \quad (5)$$

## II. Linear Alternator Modeling Using Sage

### A. Sage Linear Alternator Modeling Using the Sage Transducer Component

An alternator model can be created using the “transducer” component (Fig. 4) in the Sage EM library. Like a physical transducer, it converts energy from one type to another. In Sage it converts mechanical energy to electrical. The component has built in force and current connections and assumes the relationship shown in Eq. (6) and energy conservation shown in Eq. (7). The variable  $K_i$  is user-defined to match the system characteristics. In a linear motor or alternator type model,  $K_i$  is the motor constant.

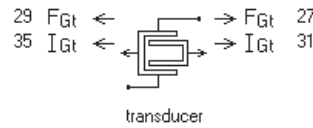


Figure 4: Sage Transducer Component

$$F = K_i * I \quad (6)$$

$$F dx/dt = \Delta VI \quad (7)$$

#### 1. Transducer Alternator Model Components

Figure (5) shows a circuit diagram of a linear alternator with controlling circuit elements.  $V_{emf}$  represents the voltage generated by the linear alternator while  $R_{alt}$  and  $L_{alt}$  represent the resistance and inductance of the alternator, respectively. The remaining resistors  $R1$  and  $R2$  are the wire and lead resistance in the circuit. A tuning capacitor is used for power factor correction and an AC power supply controls the piston amplitude. This circuit diagram is a useful comparison to the Sage model of a linear alternator using the transducer component described earlier. Figure (6) shows a Sage model of a linear alternator.<sup>18</sup> The model requires three key Sage EM components to model the linear alternator. The primary component is the transducer that converts force from the piston into electric current; however, it does not account for the resistive and inductive properties of the wire coil in the alternator. A resistor and an inductor component are needed to account for these properties. The outlined components show the key linear alternator components. The remaining components model the rest of the circuit connected to the linear alternator and compare directly to the circuit diagram.

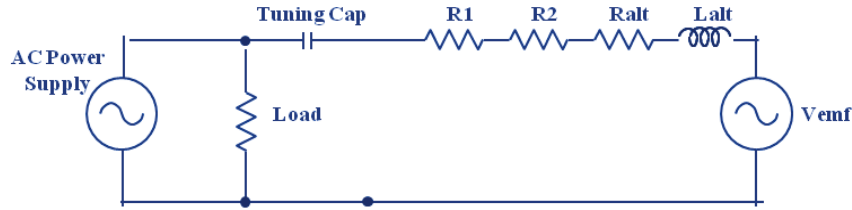


Figure 5: Circuit diagram of the linear alternator and AC bus controller.

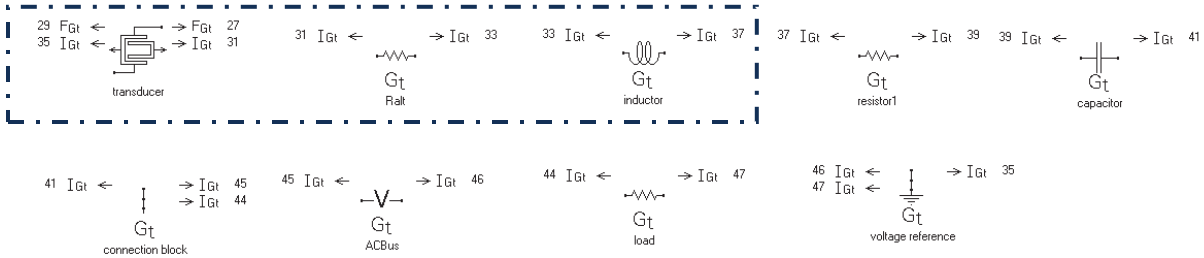


Figure 6: Linear alternator circuit model in Sage using the transducer component. Outlined are the main linear alternator model components.

## 2. Transducer Alternator Model Tuning

This method of modeling a linear alternator is simple to implement, requiring only three components, but is limited in that it ignores the underlying physical phenomena and potential losses such as eddy-currents, hysteresis, and flux leakage. It also requires that the user have data to input properties such as alternator inductance and resistance as well as the motor constant  $K_i$ . For the ASC, values for alternator inductance and resistance are known. In an attempt to account for losses, an additional resistor  $R_{loss}$  is added in the Sage model, though this assumes the losses are proportional to current. Determining an appropriate resistive loss is not straightforward as the real losses may change with convertor operation point. The same could be true for  $K_i$ .

The Sage optimization tool can be used to investigate appropriate values for  $R_{loss}$  and  $K_i$ . An estimate value for both can be input into Sage and then set as optimization variables. Constraints can be set on output variables and an objective function defined for Sage to achieve by varying the values of  $R_{loss}$  and  $K_i$ . Using performance data from the ASC, current and voltage output values are constrained to be within 2.5% of measured values and the objective function set to match the measured power factor. This was performed at four boundary operating points for the ASC known as beginning of mission (BOM) and end of mission (EOM) with high and low reject (HR and LR) temperatures at each case. The results of these optimization cases show the values for  $R_{loss}$  and  $K_i$  vary slightly across the four operation points, but a correlation can be made with the  $K_i$  value and rejection temperature (Fig. 7). This is not unexpected as the transducer and  $R_{loss}$  components do not model changes in performance due to temperature. Using this correlation, the value of  $K_i$  was input into Sage as a function of rejection temperature and the simulation repeated over the test points.

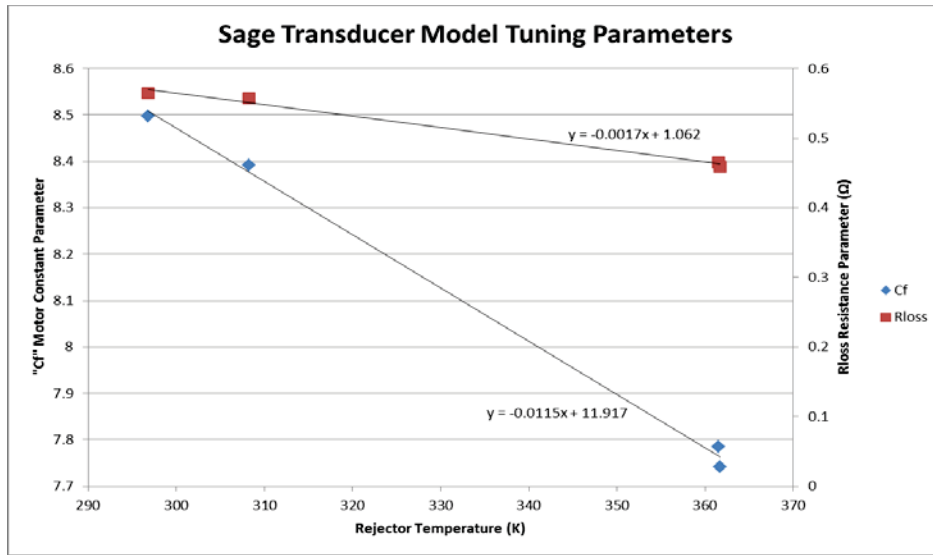


Figure 7: Transducer Tuning Parameter Value as a Function of Rejector Temperature

### B. Sage Linear Alternator Modeling with Electromagnetic Components

Creating a linear alternator model with EM components is more complex than the “transducer model”, but offers the advantage of modeling the physical characteristics of the system from first-principles. The high-level Sage EM components that model the linear alternator include a two-pole magnetic gap, a wire coil, ferromagnetic cores, and magnetic reference and connection blocks. These components are generated with the necessary magnetic flux boundary interfaces and are connected as shown in Fig. 8. The component layout in Sage does not visually represent a linear alternator, so it is important to understand the underlying physics that Sage is attempting to model.

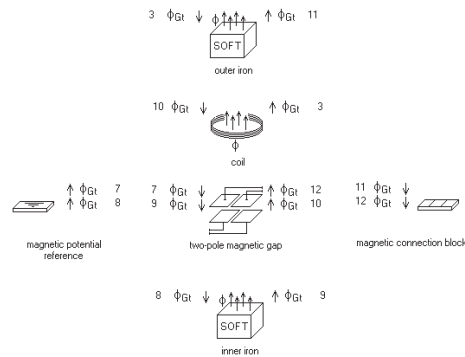


Figure 8: Sage Linear Alternator High-level Components

#### 1. Sage EM model connections and solution method

Magnetic components such as permanent magnets, magnetic poles or gaps, and ferromagnetic materials are connected through magnetic flux ( $\phi$ ) boundary interfaces that are a function of the magnetic potential difference (or magneto-motive force) across each component. Each component defines the relationship between magnetic flux and magneto-motive force based on the magnetic properties of the component. The wire coil component has both current and magnetic flux connections and the magnetic pole components have both force and magnetic flux connections. These components make it possible to model energy conversion from mechanical to EM and enable whole convertor modeling.

The Sage solution framework for EM models is based on a magnetic circuit approach. If the magnetic flux within a system is confined to a well-defined path, then the system may be understood as a magnetic circuit<sup>17</sup>, analogous to current confined to wires and components in electric circuits. Table I lists the key magnetic properties and their corresponding analogous electric properties.

**Table I: Magnetic and Electric Analogous Terms**

Magnetic Property	Electric Property
$\mathcal{F}$ = Magneto-motive force (mmf) (Amp-turns)	$V$ = Electromotive force (emf) (V)
$\phi$ = Magnetic flux (Wb)	$I$ = Electric current (A)
$\mathcal{R}$ = Magnetic reluctance ( $H^{-1}$ )	$R$ = Electric Resistance ( $\Omega$ )
$\mu$ = Permeability	$\sigma$ = Conductivity

In the magnetic circuit analogy, the magnetic system can be modeled as an electric circuit. Figure 9 shows an EM system and its corresponding electric circuit. In this example the coil produces the magneto-motive force  $\mathcal{F}$  and a magnetic flux  $\phi$  “flows” through the system. It should be noted that “flow” is merely a continuation of the electric circuit analogy as current flows through a circuit, but nothing is actually flowing through the magnetic system. The reluctance in the magnetic system due to the ferromagnetic core and air gap are analogous to resistors in an electric circuit. With this analogy, the system model can be solved using Eq. (8), which corresponds to Ohms law.

$$\mathcal{F} = \phi \mathcal{R} \quad (8)$$

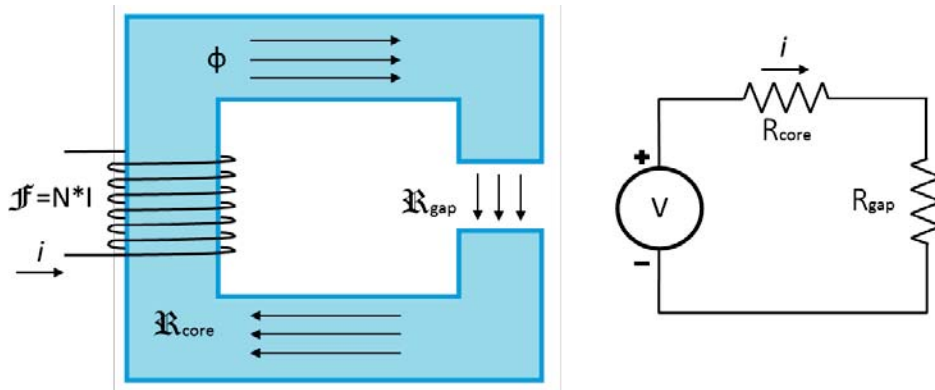


**Figure 9: Magnetic Circuit Analogy**

## 2. Properties of Sage EM Components and Sub-components

The input properties of the Sage EM components are based on the basic geometry of the alternator and relationship between components. Figure 10 shows the generic axisymmetric structure assumed in the Sage alternator model. The two-pole magnetic gap component defines the overall framework of the alternator including the length of the poles, separation between poles ( $x$  directed, along the axis), and the magnetic gap between pole faces ( $z$  directed, perpendicular to the axis). Sub-components with the two-pole component include an “EM container” which can hold permanent magnet or ferromagnetic component (for moving magnet or moving iron types of magnetic systems). The sub-components model the magnetic material, dimensions, and initial conditions such as temperature and position. Along with the magnetic flux interfaces generated from the magnetic poles is a force interface to the magnet (EM container) to connect with force interface of the piston.

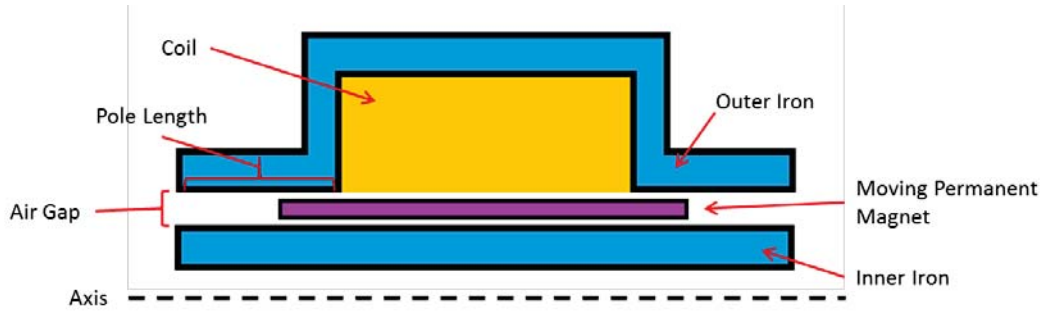


**Figure 10: Linear Alternator Generic 2-D Cross Section Assumed by Sage**

The inner and outer iron components in the model are based on the ferromagnetic material used for the alternator core and its effective magnetic path length and area. The coil component models the physical coil wire parameters such as number of turns, wire cross-sectional area, coil cross-sectional area, and coil average diameter. Coil resistance is an output parameter calculated based on wire dimensions, material properties and temperature. Coil inductance is also an output parameter that is calculated (Eq. (8)) rather than being an input parameter. The inductance can be shown to be governed by the physical dimensions of the coil and magnetic properties of the iron core. In the case of the alternator, the coil area is constant and the magnetic flux linkage can be simplified to Eq. (9) where “A” is the area of the coil and “l” is the length of the coil. The inductance of the alternator can then be defined by its physical properties (Eq. (10)) from its initial definition (Eq. (4))<sup>17</sup>.

$$\varphi = \frac{\mu N^2 A}{l} I \quad (9)$$

$$L = \frac{d\varphi}{dI} = \frac{\mu N^2 A}{l} \quad (10)$$

### 3. Sage EM Material Properties

The Sage EM library includes a selection of ferromagnetic and permanent magnet materials with typical material properties. Material properties can be edited or new materials added based on the requirements of the model. The manner that material properties are defined in Sage and assumptions made about the materials are important to the performance of the model.

Permanent magnet material properties are defined by the intrinsic (J(H)) and normal (B(H)) demagnetization curves as show in Fig. 11, where J is magnet polarization (SI unit Tesla), B is the magnetic flux density (SI unit Tesla), and H magnetizing force (SI unit Amperes per meter). Sage uses the J(H) curve end points (residual magnetic flux  $B_r$  and magnetization coercive force  $H_{cj}$ ) as inputs and uses a curve fitting term to match the demagnetization bend. Magnetic characteristics are temperature dependent so Sage allows inputs at multiple temperature points and otherwise assumes a linear relationship based on the Curie temperature.

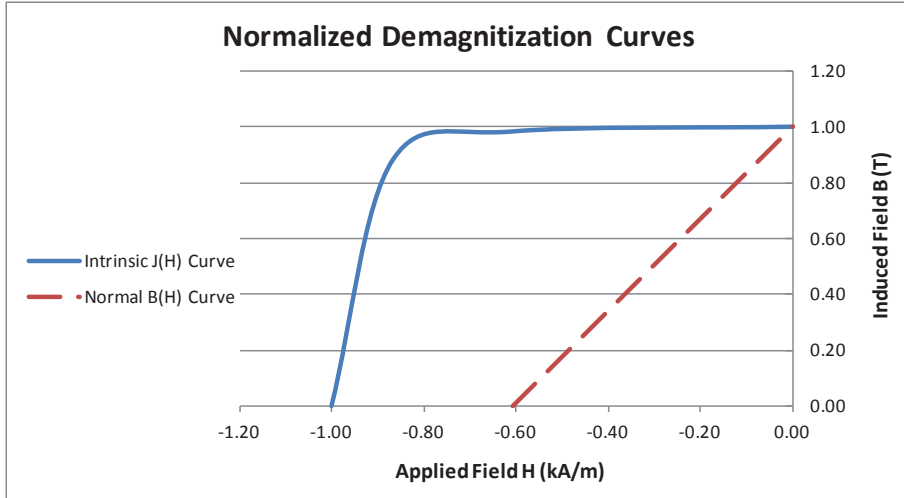


Figure 11: Permanent Magnet Demagnetization Curves (second quadrant of hysteresis loop)

Sage defines ferromagnetic material properties similarly to PM materials using critical points of the  $J(H)$  curve of the material. The saturation magnetic polarization ( $J_{Sat}$ , SI unit Tesla) and the induction coercive force (SI units Amperes per meter) are input at a specified temperature. Multiple points can be input for different temperatures if the data exist, otherwise Sage assumes a linear decrease to zero at the Curie temperature. The maximum relative permeability ( $\mu_r$ ) is also specified. Sage provides ferromagnetic material  $B(H)$  mapping model to allow comparison and tuning of the  $B(H)$  curve of the material. Figure 12 shows a comparison of the  $B(H)$  curve from test data and the  $B(H)$  curve generated in Sage from data. This comparison allows for a “tuned” value for  $\mu_r$  and  $J_{Sat}$  to be found and the  $B(H)$  curve to be matched.

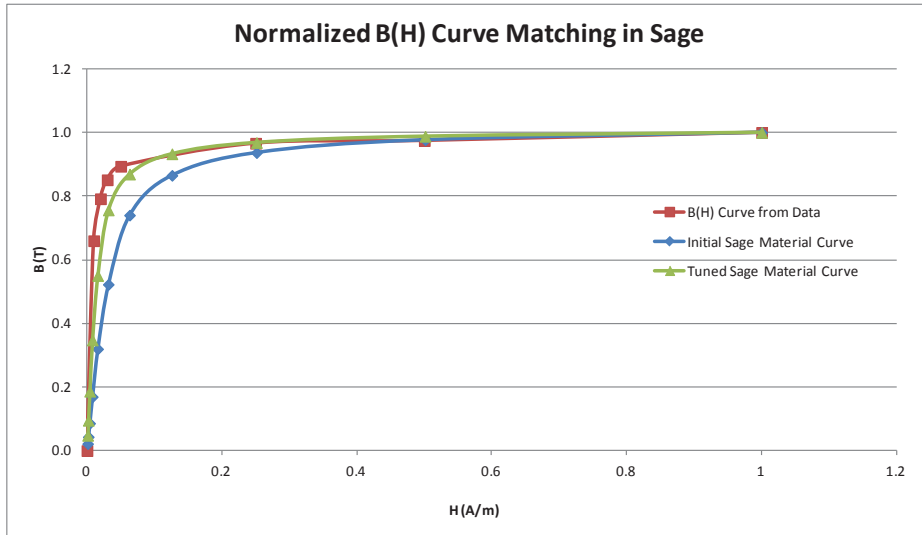


Figure 12:  $B(H)$  Curve Matching in Sage for Ferromagnetic Core Material

### C. Sage EM Alternator Model Tuning

The Sage alternator model is a 1-D model and assumes all input geometry is symmetric about its axis. This assumption works well but is not entirely accurate as manufacturing and assembly constraints can cause some non-symmetric features, such as the outer iron core laminations not forming a continuous covering. The dimensions of the alternator are also idealized as shown previously in Fig. 10. Actual alternator geometry is more complex. This may produce some inaccuracies due to Sage overestimating or underestimating parameters such as amount of iron

core material and magnetic path length and area. This can affect the magnetic circuit model by altering the magnetic reluctance of components or altering magnetic flux through components by inaccurate area calculations.

Another source of error in the EM model is from magnetic fringe field effects across the magnetic gaps at the poles of the alternator. Fringing flux occurs at gaps in the ferromagnetic path allowing the magnetic field to bulge outwards. Sage models fringing flux similarly to an electric field in a parallel plate capacitor, as the governing equations are similar and fringe fields in capacitors are well studied.<sup>14</sup> It is also possible that not all of the windings of the alternator coil enclose the same amount of magnetic flux as Sage assumes. Figure 13 shows a 2D plot of flux through an alternator (created with the Maxwell FEM software package) with the PM off-center, showing the presence of fringing fields and field lines in the inner core not uniformly distributed along the length of the coil windings.

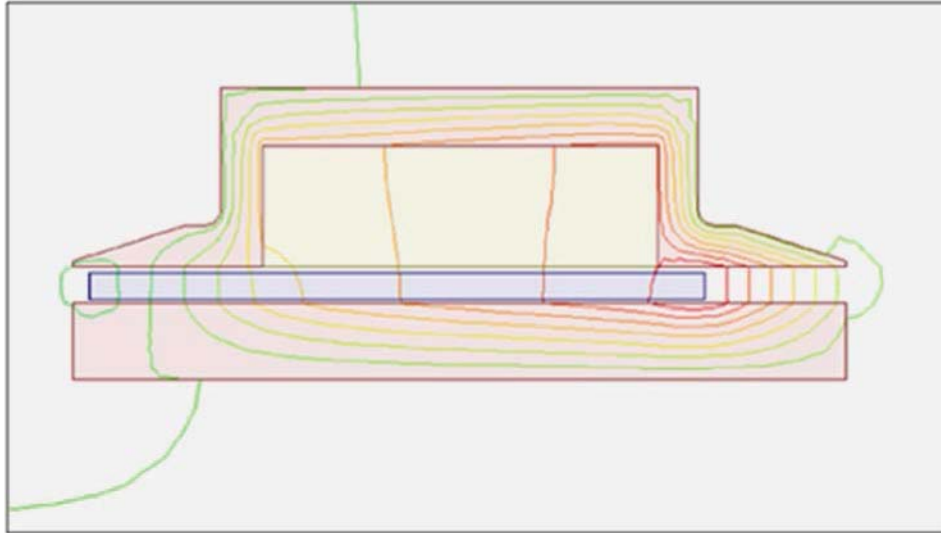


**Figure 13: 2-D Magnetic Flux Plot of a Linear Alternator**

### 1. Tuning Parameters

Sage has two built-in tuning parameters to address the known limitations of modeling using the EM components. There is a multiplier parameter “FringeMult” that directly scales the effect of fringing fields at the magnetic poles of the model. There is a second multiplier term “Jmult” that scales the strength of the PM. This can account for any demagnetization that may have occurred to the magnet during operation or reflect real magnet strength values less than those presented in the material data sheet. These terms together may also act to correct for other modeling inaccuracies such as geometry or magnetic flux path idealizations.

Certain parameters may also be altered in tuning of the alternator model to compensate for some of the inaccuracies in the model. The overall magnetic path length and area of the alternator may be modified to reflect the effective area of the iron cores that may not be accurately modeled in the axisymmetric assumption. Another possible parameter that could be used is the air gap dimension defining the distance between pole faces. Altering this distance ( $l_{gap}$ ) changes the magnetic reluctance of the magnetic circuit as seen in Eq. (11).

$$\mathfrak{R} = \frac{l_{gap}}{\mu A} \quad (11)$$

### 2. Alternator Model Inductance Test and Verification

The inductance of the alternator directly impacts performance and is governed by the overall geometry of the coil and iron cores. Testing and tuning the Sage alternator model to match the measured inductance of alternator acts to increase confidence in the model’s physical parameters. As the coil parameters (number of turns, resistance, dimensions, etc.) are well known and modeled accurately, it is the permeance (inverse of reluctance) of the magnetic

path that may require tuning. The relationship between inductance and reluctance in a magnetic circuit (Eq. (12)) can be shown by substituting Eq. (4) into Eq. (5) and simplifying.

$$L = \frac{N^2}{\mathfrak{R}_{total}} \quad (12)$$

To check the inductance of the alternator model, a separate model was created with the identical alternator inputs. This alternator model was set up with a current source attached to the alternator and the piston stationary with magnets centered in the alternator. This was to mimic the inductance test performed on the linear alternator during the manufacturing process. A large current was input in the model and the inductance was reported in the Sage output listing.

### 3. Alternator Model Performance Tuning using Maxwell Model Simulation

The performance of the Sage EM alternator model was compared against a Maxwell FEM model of the alternator. This comparison served to examine the accuracy of a 1-D Sage EM model compared to the 3-D FEM model as well as to provide simulated alternator performance data for tuning purposes, in the absence of stand-alone alternator test data. The main tuning parameter tested in this process was the “Jmult” term. This tuning was re-evaluated in the integrated ASC model, combining the new Sage EM alternator model with the Stirling engine model, and the “Jmult” term adjusted.

## III. Simulation Results and Model Validation

The Sage transducer model and EM model were combined with the ASC model and tuned at four key operating conditions (BOM-LR, BOM-HR, EOM-LR, and EOM-HR). Simulations using the tuned models at these operating points were compared to measured data from convertor verification testing conducted at Sunpower. After convertor verification testing at Sunpower, the position sensor attached to the displacer was removed before the ASC was placed on extended testing at NASA GRC. This slightly changes the mass of the displacer, so displacer mass in the Sage model was adjusted and simulations were compared to performance map tests conducted at GRC.

### A. Sage ASC with Transducer Alternator Model Results

Table II displays the parameters measured, the BOM and EOM operating conditions, and the percent error between the tuned Sage ASC with transducer alternator model simulation and measured data points. Piston amplitude was matched as an input parameter for each case. The model agrees with measured data within 5% or better on most parameters.

**Table II: Sage Transducer Model Percent Error to Test Data, BOM/EOM Point Comparison**

Test Parameters Sage Transducer Alternator Model	BOM-LR	BOM-HR	EOM-LR	EOM-HR
Net-heat input, Q (W)	2.29%	-2.14%	5.37%	-2.36%
Piston Amplitude (mm)	0.00%	0.00%	0.00%	0.00%
Displacer Amplitude (mm)	0.73%	1.30%	0.82%	0.85%
Displacer to Piston Phase (degree)	1.01%	0.11%	2.03%	0.38%
Piston to Current Phase (degree)	-0.11%	2.30%	-1.51%	1.92%
Terminal power (W)	-0.27%	0.38%	0.64%	-0.46%
Power factor	0.21%	-0.43%	0.25%	0.30%
Voltage rms (V)	-2.64%	-2.43%	-1.18%	-2.78%
Current rms (A)	2.08%	2.38%	2.01%	2.37%
Efficiency (%)	-2.51%	2.58%	-4.49%	1.95%

The model was updated to include the change in displacer mass and simulations compared to performance map data performed at GRC. Figure 14 shows convertor efficiency at constant input temperature and varied rejector temperature. Piston amplitude was also varied in the test data. The Sage model was operated at the same input temperature and piston amplitude as the test data. The values beside each data point are the net heat input, Q. The Sage model trends similarly with a net heat input difference less than +5%. Figure 15 show the same performance

map data set plotted as power output vs. rejector temperature. It can be seen here the Sage model under predicts power output by 3%. The model's under prediction of power output and over prediction of heat input leads to the variance seen in conversion efficiency.

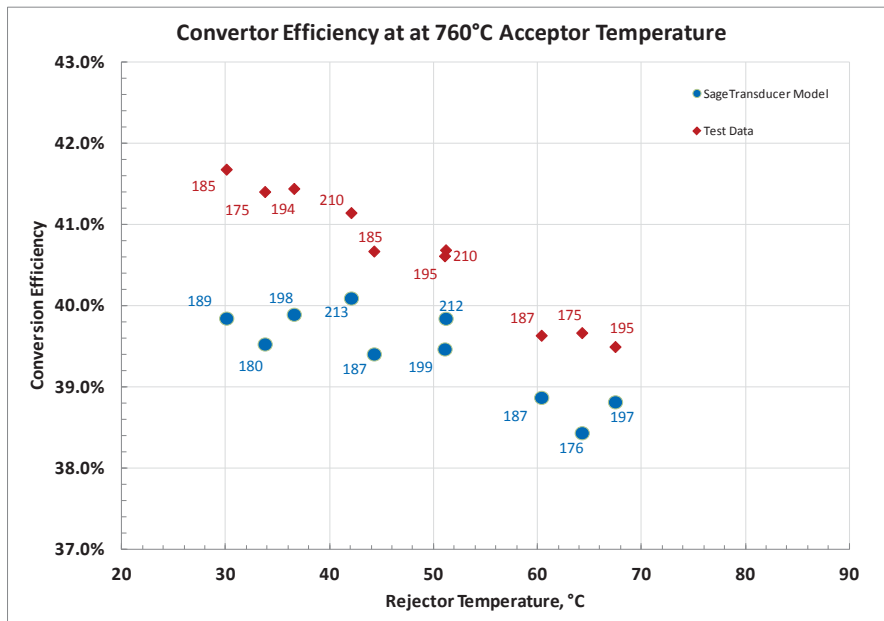


Figure 14: Sage ASC Model with Transducer Alternator, Comparison of Convertor Efficiency

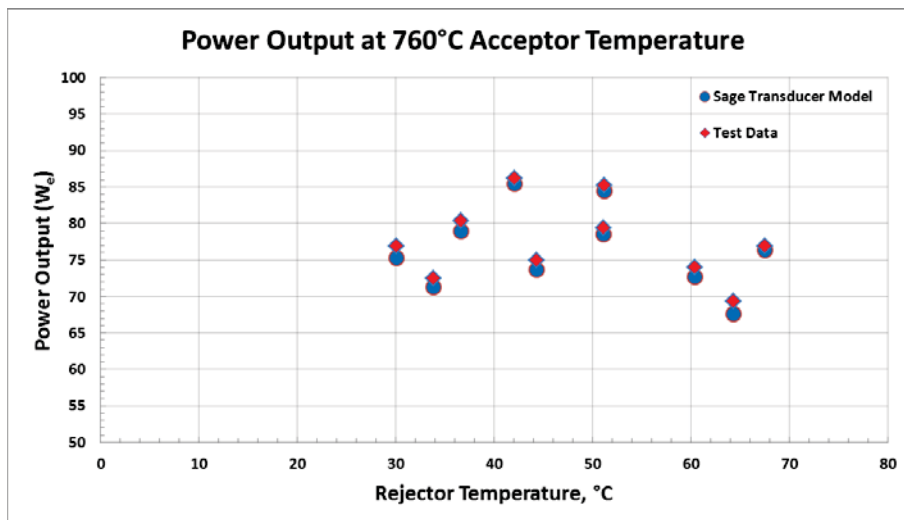


Figure 15: Sage ASC Model with Transducer Alternator, Comparison of Power Output

### B. Sage ASC with EM Alternator Model Results

The Sage ASC model with EM alternator is operated at the BOM and EOM operating conditions and compared with measured data. Table III displays the parameters measured at the BOM and EOM operating conditions and the percent error between the model simulations and measured data. Acceptor and rejector temperatures were set as inputs and piston amplitude was matched within 0.05%. The model was tuned at the BOM-LR operating conditions and agreed with measured data within 2%. The model agrees with the remaining operating points within 6% or better.

**Table III: Sage EM Model, BOM/EOM Point Comparison**

Test Parameters Sage EM Alternator Model	BOM-LR	BOM-HR	EOM-LR	EOM-HR
Net-heat input, Q (W)	-1.03%	-5.07%	1.92%	-5.45%
Piston Amplitude (mm)	0.00%	0.05%	-0.05%	-0.05%
Displacer Amplitude (mm)	-1.40%	-0.92%	-1.36%	-1.56%
Displacer to Piston Phase (degree)	-0.89%	-1.26%	-0.02%	-0.94%
Piston to Current Phase (degree)	0.44%	1.87%	-0.80%	1.92%
Terminal power (W)	0.44%	-3.96%	3.92%	-4.72%
Power factor	0.46%	1.45%	-0.63%	3.43%
Voltage rms (V)	-0.85%	-5.02%	2.57%	-5.32%
Current rms (A)	0.89%	-1.75%	1.70%	-2.37%
Efficiency (%)	1.48%	1.16%	1.96%	0.77%

The model was updated to account for the change in displacer mass and simulations compared to performance map data gathered at GRC. The simulations matched the acceptor and rejector input temperatures and piston amplitude. Figure 16 shows the convertor efficiency with varied rejector temperature and piston amplitude. Net heat input, Q, is displayed next to each data point. Convertor efficiency in the model simulations corresponds to test data within 2%.

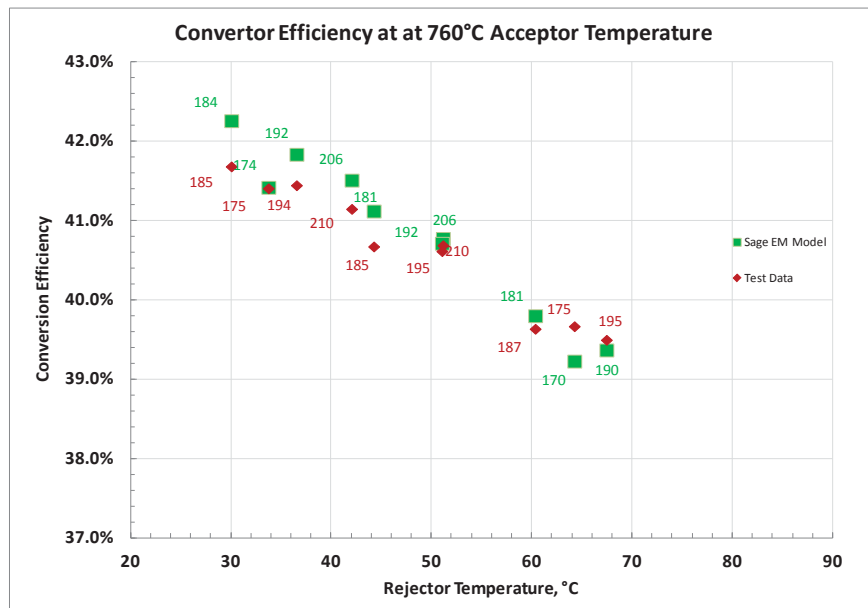


**Figure 16: Sage ASC Model with EM Alternator, Comparison of Convertor Efficiency**

Figure 17 compares power output of the EM model simulations against test data. The model agreed well with the test data at low reject temperatures, but the difference increases with increasing rejector temperature. This indicates that the model may not accurately account for temperature effects in the alternator, such as reduced magnetic saturation in the iron core or reduced magnet strength with increasing temperature. Even at high rejection temperature though, the model still agreed with test data within 5 percent.

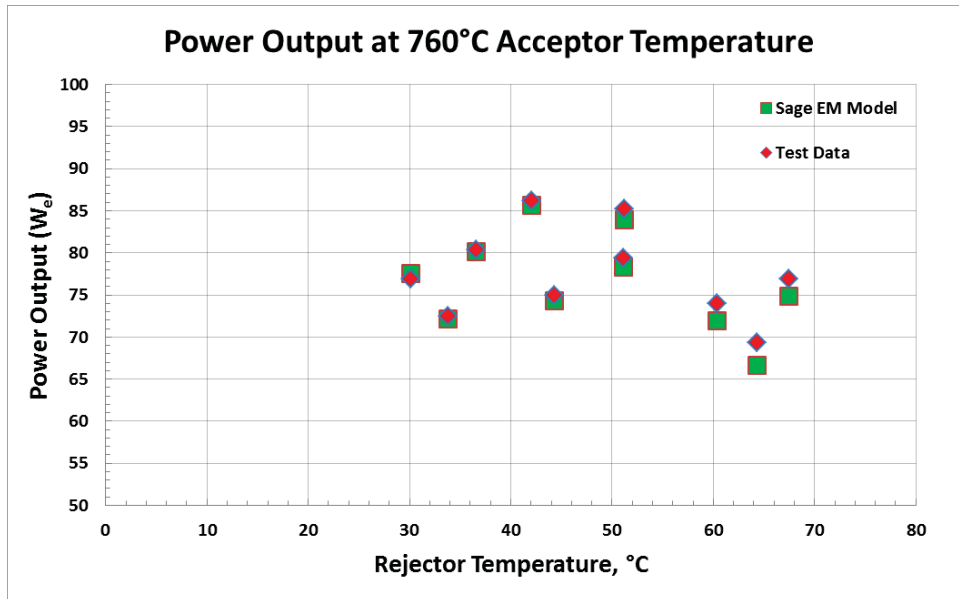


Figure 17: Sage ASC Model with EM Alternator, Comparison of Power Output

### C. Sage Alternator Model Comparison

Figure 18 compares converter efficiency the Sage transducer model and EM model of the alternator against each other at their default (un-tuned) and tuned configurations when simulated at the BOM/EOM operating points. The default EM alternator model matches the data better than the default transducer model and almost as well as the tuned models. A plot displaying model comparison of power output (Fig. 19) shows similar results, though it should be noted that other parameters such as voltage, current, and power factor vary more in the default models (up to 20% error in the un-tuned models).

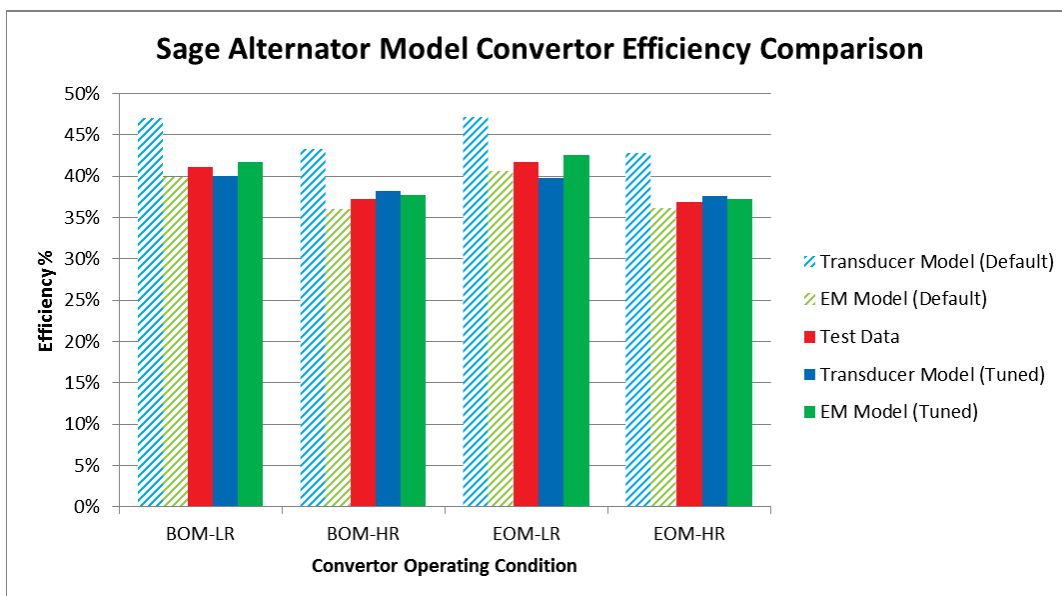


Figure 18: Sage Alternator Model Comparison of Converter Efficiency

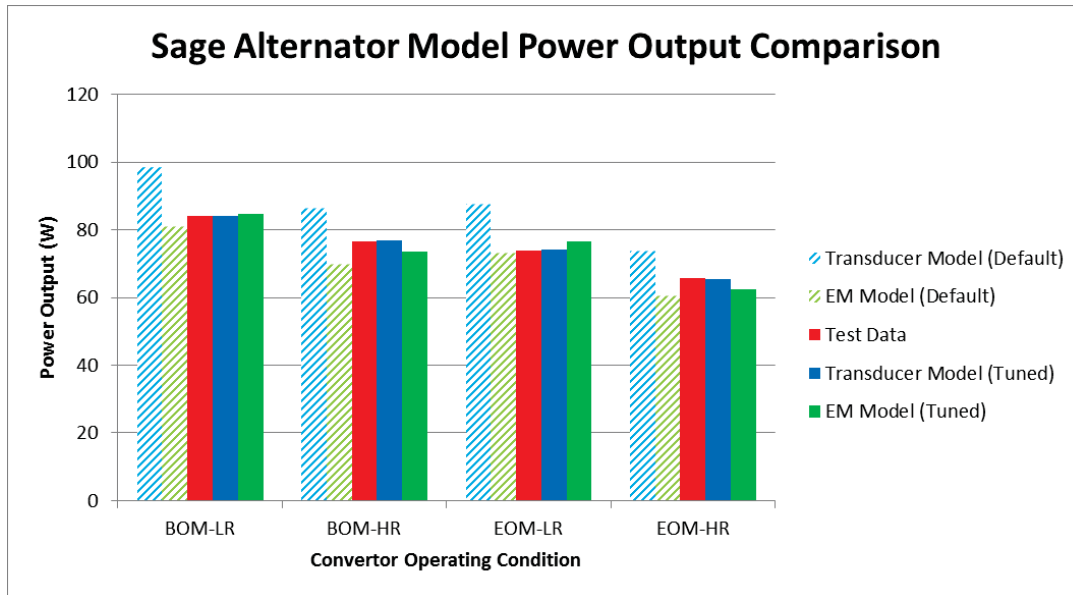


Figure 19: Sage Alternator Model, Power Output Comparison

#### IV. Conclusion

Two methods of modeling a linear alternator using the Sage 1-D modeling software were presented and used to create a more complete system model of the ASC. The models were tuned to BOM/EOM operating conditions using Sunpower data and simulation results were within about 5% of measured ASC performance. The models were then used in a performance mapping simulation and agreed with separate test data gathered at GRC within 5%. The transducer alternator model is the simpler model to implement but requires test data over a range of operating points to determine appropriate motor constant and loss parameters. The EM model is created from physical parameters of the alternator and does not require test data to perform preliminary simulations. This enables the EM model to be useful in the design of alternators as well as being able to tune it to test data. Using the Sage software to create a 1-D whole convertor model of the ASC allow for simulations of steady-state convertor performance without the more computationally intensive 3-D models.

#### Acknowledgments

This work was funded with the support of the NASA Science Mission Directorate and the Radioisotope Power Systems Program Office. Any opinions, findings, conclusions, or recommendations expressed in this article are those of the authors and do not necessarily reflect the views of NASA.

#### References

- <sup>1</sup>Thieme, Lanny G., Jeffrey G. Schreiber, and Lee S. Mason. *Stirling technology development at NASA GRC*. National Aeronautics and Space Administration, Glenn Research Center, 2001.
- <sup>2</sup>Richardson, R. and Chan, J., "Advanced Stirling Radioisotope Generator," Proceedings of NASA Science Technology Conference (NSTC 2007)
- <sup>3</sup>Wood, J.G, and Carrol, Cliff. "Advanced Stirling Convertor Program Update," in *Proceedings of the Second International Energy Conversion Engineering Conference (IECEC 2004)* American Institute for Aeronautics and Astronautics, 2004.
- <sup>4</sup>Wong, W.A., Wilson, K., Smith, E., and Collins, J. "Pathfinding the Flight Advanced Stirling Convertor Design with the ASC-E3," in *Proceedings of the Tenth International Energy Conversion Engineering Conference (IECEC 2012)* American Institute for Aeronautics and Astronautics, 2012.
- <sup>5</sup>Williams, Zachary D., and Oriti, Salvatore M. "Advanced Stirling Convertor (ASC-E2) Characterization Testing," in *Proceedings of the Tenth International Energy Conversion Engineering Conference (IECEC 2012)* American Institute for Aeronautics and Astronautics, 2012.

<sup>6</sup>Oriti, Salvatore M. "Performance Measurement of Advance Stirling Convertors (ASC-E3)," in *Proceedings of the Eleventh International Energy Conversion Engineering Conference (IECEC 2013)* American Institute for Aeronautics and Astronautics, 2013.

<sup>7</sup>Dyson, Rodger W., Scott D. Wilson, and Roy C. Tew. "Review of Computational Stirling Analysis Methods," in *Proceedings of the Second International Energy Conversion Engineering Conference (IECEC 2004)* American Institute for Aeronautics and Astronautics, 2004.

<sup>8</sup>Lewandowski, E.J., and Regan, T.F., "Overview of the GRC Stirling Convertor System Dynamic Model," in *Proceedings of the Second International Energy Conversion Engineering Conference (IECEC 2004)*, American Institute of Aeronautics and Astronautics, 2004.

<sup>9</sup>Ebiana, A. B., Savadekar, R.T., Vallury, A. "2<sup>nd</sup> Law Analysis of Sage and CFD-ACE+ Models of MIT Gas Spring and "Two-Space" Test Rigs," in *Proceedings of the Second International Energy Conversion Engineering Conference (IECEC 2004)* American Institute for Aeronautics and Astronautics, 2004.

<sup>10</sup>Zhang, Zhiguo and Ibrahim, Mounir. "Development of CFD model for Stirling Engine and its Components," in *Proceedings of the Second International Energy Conversion Engineering Conference (IECEC 2004)* American Institute for Aeronautics and Astronautics, 2004.

<sup>11</sup>Dyson, Rodger W., Wilson, Scott D., Tew, Roy C., and Demko, R. "On the Need for Multidimensional Stirling Simulations," in *Proceedings of the Third International Energy Conversion Engineering Conference (IECEC 2005)* American Institute for Aeronautics and Astronautics, 2005.

<sup>12</sup>Geng, Steven M., and Schwarze, Gene E. "A 3-D Magnetic Analysis of a Linear Alternator for a Stirling Power System," in *Proceedings of the 36<sup>th</sup> Intersociety Energy Conversion Engineering Conference (IECEC 2001)*, Savannah, GA, 2001.

<sup>13</sup>Gedeon, David. "Sage: Object Oriented Software for Stirling Machine Design," AIAA Paper 94-4106-CP. 1994.

<sup>14</sup>Gedeon, David. "Sage User's Guide, Ninth Edition," Gedeon Associates, 2013.

<sup>15</sup>Griffiths, D.J., *Introduction to Electrodynamics*, Prentice Hall, New Jersey, 1989.

<sup>16</sup>Halliday, David, and Resnick, Robert, *Fundamentals of Physics*, 2<sup>nd</sup> ed., John Wiley & Sons, New York, 1986, Chaps.32-34.

<sup>17</sup>Reitz, J.R., Milford, F.J, and Christy, R.W., *Foundations of Electromagnetic Theory*, 3<sup>rd</sup> ed., Addison-Wesley Publishing Company, Inc., Reading, MA, 1980, Chaps. 9-12.

<sup>18</sup>Metscher, Jonathan F., and Lewandowski, Edward J. "Development and Integration of an Advanced Stirling Convertor Linear Alternator Model for a Tool Simulating Convertor Performance and Creating Phasor Diagrams," in *Proceedings of the Eleventh International Energy Conversion Engineering Conference (IECEC 2013)* American Institute for Aeronautics and Astronautics, 2013.